Available online at www.sciencedirect.com
SCIENCE DIRECT®
Organic Electronics 5 (2004) 315–320
Organic Electronics
www.elsevier.com/locate/orgel

Optical constants and self-assembly of phenylene ethynylene oligomer monolayers

Eike Marx [a], Karsten Walzer [b], Robert J. Less [c], Paul R. Raithby [c], Kurt Stokbro [b], Neil C. Greenham [a,*]

[a] *Cavendish Laboratory, University of Cambridge, Madingley Road, Cambridge CB3 0HE, United Kingdom*
[b] *Mikroelektronik Centret (MIC), Technical University of Denmark, Bldg. 345 east, DK-2800 Lyngby, Denmark*
[c] *Department of Chemistry, University of Bath, Bath BA2 7AY, United Kingdom*

Received 23 June 2003; received in revised form 24 March 2004; accepted 19 October 2004
Available online 20 November 2004

Abstract

This paper studies the self-assembly on gold surfaces of 1,4-ethynylphenyl-4′-ethynylphenyl-2′-nitro-1-benzenedithiolate ($EP2NO_2$), a substituted phenylene ethynylene trimer with applications in molecular electronics. We develop an ellipsometric technique to measure the optical constants of these self-assembled monolayers, and we also use attenuated total reflection Fourier transform infrared (ATR-FTIR) spectroscopy and scanning tunneling microscopy (STM) to confirm the structure of the films.

PACS: 78.20.C
Keywords: Optical constants; Optical ellipsometry; Self-assembly; Phenylene ethynylene oligomers

1. Introduction

The emerging field of molecular-scale electronics (molecular electronics) is based on measuring the electrical properties of individual molecules, or of a number of individual molecules in parallel. Self-assembled monolayers of conjugated molecules have been shown to exhibit negative differential resistance and memory effects, which have potential applications in ultrafast electronics [1,2]. In order to control the fabrication and operation of these devices, it is important to obtain a detailed understanding of the self-assembly of conjugated molecules and the properties of the resulting films. In previous studies, Tour and co-workers [3,4] have described the self-assembly of different conjugated thiols, dithiols and thiolacetyls, and Duan and Garrett [5] have investigated

* Corresponding author. Tel.: +44 1223 766301; fax: +44 1223 353397.
E-mail address: ncg11@cam.ac.uk (N.C. Greenham).

1566-1199/$ - see front matter
doi:10.1016/j.orgel.2004.10.005

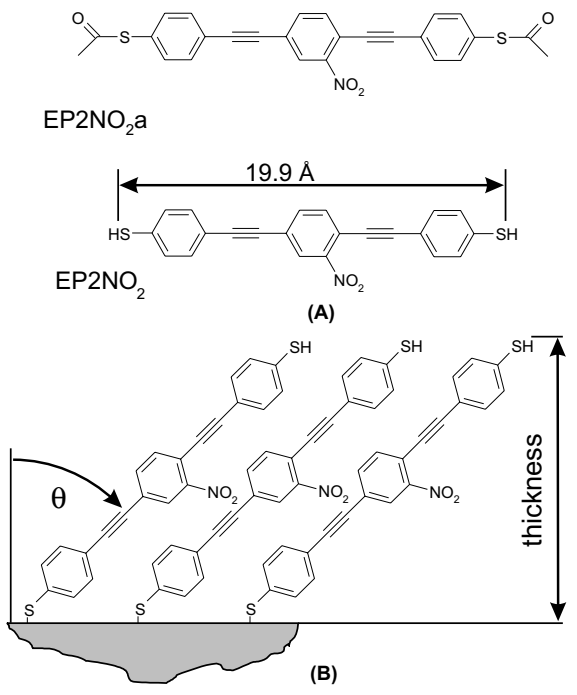

Fig. 1. Schematic illustration of (A) the molecule before self-assembly, and (B) the SAM on the Au substrate.

the self-assembly of *p*-methylterphenyl thiol on Au(1 1 1) substrates. Here, we present a detailed study of the properties of films of 1,4-ethynylphenyl-4′-ethynylphenyl-2′-nitro-1-benzene-dithiolate ($EP2NO_2$) assembled on gold substrates. This substituted phenylene ethynylene trimer (Fig. 1) has been shown to exhibit negative differential resistance at room temperature [2]. We use attenuated total reflection Fourier transform infrared (ATR-FTIR) spectroscopy, optical ellipsometry, scanning tunneling microscopy (STM), and UV–visible (UV–vis) spectroscopy to characterize the films, and we develop ellipsometric methods which take into account the effect of conjugation on the optical constants of the molecules.

2. Sample preparation

$EP2NO_2$ was synthesized using methods described previously [6]. The product was obtained as the thioacetyl derivative $EP2NO_2a$ (as shown in Fig. 1), and the thioacetyl end groups were selectively hydrolyzed to form free thiol end groups during the self-assembly, as has been reported previously. The molecules were self-assembled on Au(1 1 1) substrates or on semitransparent Au substrates. The self-assembly on Au(1 1 1) substrates was performed following a routine described by DeRose et al. [7]. Freshly cleaved muscovite mica was inserted into high vacuum (10^{-6} mbar) and annealed for 24 h at 500 °C. Subsequently, ~200 nm Au was thermally evaporated onto the hot substrate, and annealed for 1 h at 500 °C. Immediately afterwards, the substrates were exposed to a solution containing 0.1 mM $EP2NO_2a$ in tetrahydrofuran (THF, Acros Organics, purity >99.5%) and 500:1 aqueous ammonia (Aldrich, 25%, or Gruessing, 25%) in the dark for 21 h [6]. After assembly the samples were thoroughly rinsed with pure THF. Semitransparent Au substrates were fabricated by thermal evaporation of ~2.5 nm Cr and ~7 nm Au onto a quartz substrate (Spectrosil B, UQG Optics, UK). To form the SAM, the substrates were exposed to a solution containing the same concentration of $EP2NO_2a$, ammonia and THF (or acetonitrile) for 48 h in darkness and at room temperature. All samples were kept under nitrogen to prevent oxidization before the measurements were made.

3. Results and discussion

The presence of $EP2NO_2$ molecules on the Au(1 1 1) substrate was investigated by ATR-FTIR measurements, which were performed using a Nicolet 5SXB FTIR in combination with a Specac ATR accessory, and gave a resolution of 4 cm^{-1}. Fig. 2 shows the spectra both for self-assembled films of $EP2NO_2$, and for $EP2NO_2a$ powder. The powder shows peaks at 2981 cm^{-1} and 2887 cm^{-1}, corresponding to radial C–H stretching vibrations in benzene rings containing different substituents. For the SAM, the spectrum showed peaks at 2857 cm^{-1}, 2927 cm^{-1} and 2955 cm^{-1}. The shift of the C–H stretching modes to lower energy is consistent with enhanced intermolecular interactions due to close-packing in the SAM [8,9]. The additional peak at high energy may also be due to the effect of intermolecular interactions.

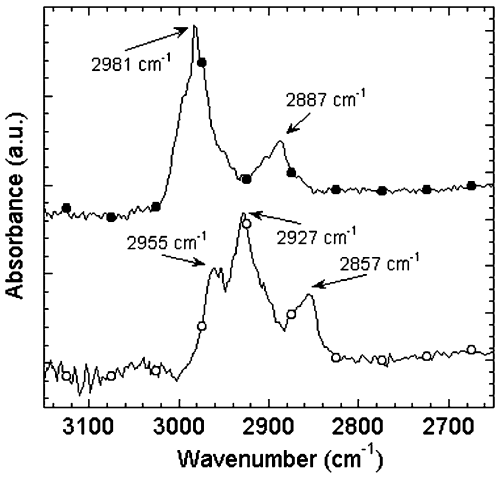

Fig. 2. ATR-FTIR spectra of the SAM (○) and of the bulk material (●).

Fig. 3 shows the UV–vis absorption spectra of $EP2NO_2a$ in solution, and of a self-assembled monolayer of $EP2NO_2$. A π–π* absorption peaking at 323 nm is clearly visible. The SAM spectrum was measured by comparing transmission spectra for semitransparent gold substrates with and without assembly of $EP2NO_2$, however it was difficult completely to remove reflection effects in the spectra of these weakly-absorbing films, especially in the region of the absorption onset. Nevertheless, the spectra are very similar, consistent with the absence of strong additional electronic interactions between neighboring molecules in the SAM. This indicates that, despite the close packing implied by the infrared spectra, there is negligible ground-state electronic wavefunction overlap between neighboring molecules in the SAM.

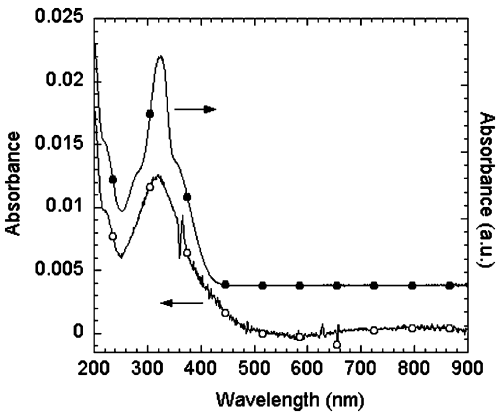

Fig. 3. Absorption of the molecules in solution as determined with UV–vis spectroscopy (●). Absorption of the molecules in the SAM on a semitransparent Au substrate (○).

Optical ellipsometry, which is used to determine layer thicknesses, measures the change of polarization of a light beam reflected by a surface as a function of its wavelength and angle of incidence. The experimentally measured values Ψ and Δ are defined by

$$\tan(\Psi)e^{i\Delta} = \frac{\widetilde{R}_p}{\widetilde{R}_s}$$

where $\widetilde{R}_p$ and $\widetilde{R}_s$ are the complex amplitude reflection coefficients for *p*- and *s*-polarized light, respectively. Determination of the optical constants and thickness of a thin film on a substrate involves constructing an optical model for the sample and iterating the parameters to obtain the best fit to the measured data. For a SAM or other ultrathin film, the independent determination of the optical constants and the thickness of the films is problematic as both are highly correlated. Previous single-wavelength ellipsometry measurements of SAMs of aliphatic or aromatic hydrocarbons assumed an index of refraction, *n*, between 1.45 and 1.55 at 632.8 nm [3,8,10]. These values, however, do not account for any conjugation in the molecules, which should be reflected in a higher index of refraction. Underestimation of the refractive index will lead to an overestimate of the film thickness. To determine more accurate optical constants and layer thicknesses, spectroscopic ellipsometry including both absorbing and non-absorbing regions of the film was used. Variable-angle spectroscopic ellipsometry was performed using a J. A. Woollam M-2000 rotating compensator ellipsometer at angles of 45°, 50°, 55°, 60° and 65° from the normal. To reduce the number of fitting parameters, the shape of the extinction coefficient spectrum was fixed to be consistent with the shape of the solution absorption spectrum. This was achieved by modeling the SAM with a combination of five Gaussian oscillators with resonance frequencies, damping factors and relative oscillator strengths adjusted to give the best fit to the absorption spectrum. Parameters for these oscillators are

Table 1
Gaussian oscillator parameters for fitting $EP2NO_2$. The imaginary part of the dielectric function is given by $\varepsilon_2 = \sum_n A_n \exp -\left(\frac{E-E_n}{\beta_n}\right)^2$ where E is the photon energy in eV

Oscillator	Resonance energy, E_n (eV)	Strength, A_n	Damping factor, β_n (eV)
1	3.40	0.70	0.27
2	3.74	0.24	0.09
3	3.88	1.45	0.28
4	4.39	0.57	0.34
5	6.90	1.79	1.76

given in Table 1. To model the real part of the refractive index, it is necessary to know the absolute strength of the oscillators in the model, and also to account for the effect of oscillators lying outside the measured wavelength range [11]. To achieve this whilst maintaining both Kramers–Kronig consistency and the shape of the absorption spectrum, the optical constants for the oscillator model were combined using the Bruggeman effective-medium approximation with a constant refractive index component ($n = 6$, $k = 0$) and a void ($n = 1$, $k = 0$) in varying proportions. The fraction of each component in the model, and the thickness of the film, were allowed to vary in order to obtain the best fit to the ellipsometric data. The void and constant refractive index components do not represent the properties of any physical component in our sample; the void fraction simply modifies the total oscillator strength in our model and the constant refractive index component allows the background dielectric constant to be accounted for. The fitting was performed between 300 nm and 500 nm using J. A. Woollam Co. WVASE32 software, which uses the Levenberg–Marquardt algorithm for optimization. The fractions obtained were 46% void, 20% constant refractive index, and 34% oscillator model with the parameters shown in Table 1.

The optical constants determined for the $EP2NO_2$ SAM are shown in Fig. 4. The thickness was determined to be 15.5 ± 0.2 Å. The correlation coefficient between n and the thickness was 0.889, sufficiently low to allow independent determination of both parameters. The mean squared error (MSE) value was 1.006, consistent with a good fit between model and experiment. The distance

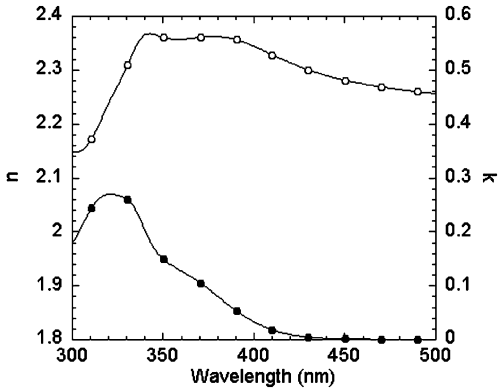

Fig. 4. Real (n, ○) and imaginary (k, ●) parts of the complex refractive index of the phenylene ethynylene trimer as determined by fitting of ellipsometry and UV–vis data.

between the two S atoms in $EP2NO_2$ has been calculated to be 19.9 Å [6], corresponding to a total length of approximately 22 Å when the interaction between the S atom and the surface is included. Assuming a tilted close-packed structure as shown in Fig. 1(B), comparing the film thickness to the total length of the molecule gives an angle to the normal, θ, of approximately 45°. The refractive index obtained (~2.32 at 633 nm) by fitting the optical constants in the wavelength region of 300–800 nm is significantly higher than for saturated SAMs, consistent with the conjugated electronic structure of $EP2NO_2$. Similarly high values for n are found in conjugated polymers [12].

Fitting over a range of wavelengths is vital to obtain satisfactorily low correlation coefficients between thickness and optical constants. The correlation coefficient decreases as the wavelength range is increased from a narrow range around 300 nm to a range of 300–500 nm. Extending the wavelength range further towards the red does not reduce the correlation further, and leads to a slight increase in the MSE due to the difficulty of modeling the sample accurately in the region where the substrate becomes strongly absorbing.

The proposed structure for the SAM implies that a degree of anisotropy is expected in the sample. It is presumed that the SAM consists of small domains, each tilted in a random direction. No change in the ellipsometric data are seen on rotating the sample about an axis normal to its plane,

implying that these domains are considerably smaller than the spot size. It is likely that the domains are smaller than the wavelengths used for ellipsometry, and hence the SAM may be described by averaging over the domains to give an effective optical constant, which exhibits uniaxial anisotropy. We find negligible depolarization in our experiments, consistent with this assumption. Our model, however, assumes an isotropic optical constant in the SAM, which will introduce some error in the modeling. Unfortunately, though, it is not possible to extract independent values of in-plane and out-of-plane optical constants for these ultra-thin films using reflection ellipsometry. Due to the small range of internal angles within the film in the ellipsometry experiment, the optical constants determined with the uniaxial model will be dominated by the in-plane optical constants. We have checked by fitting simulated anisotropic ellipsometry data that the film thickness determined using a uniaxial model is insensitive to the neglect of anisotropy.

To confirm the film thicknesses determined by ellipsometry, scanning tunneling microscopy measurements were performed on SAMs under ultra high vacuum (UHV). Details of the tunneling spectra measured have been reported elsewhere [6]. Electrochemically NaOH dc-etched tungsten tips (diameter ~20 nm) were transferred into UHV immediately after an additional etch for 1 min with 5% hydrofluoric acid. Fig. 5 shows the topography of the sample, where a high tunneling current has been used to remove the SAM in a small area, revealing the bare substrate as shown in the inset. The cross section of this area is illustrated in Fig. 5(C) showing step heights of ~1.5 nm, revealing the thickness of the SAM. The cross section exhibits the real height of the SAM as the same escape energies for electrons in the SAM and in the nearly SAM-free substrate can be assumed [6] and the tip does not touch the SAM surface as the tunneling current is very low (a few pA). The ridge (~2.5 nm) between the substrate and the SAM is caused by the deposition of molecules removed whilst forming the bare area. The step heights measured with STM suggest a tilted molecule on the surface and correspond very well with the thickness measured with ellipsometry.

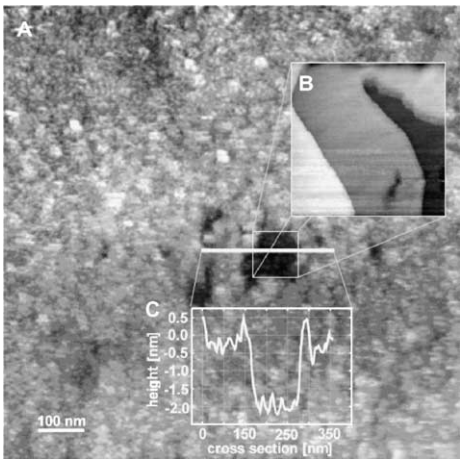

Fig. 5. (A) STM images of the SAM on the Au(1 1 1) substrates (tunneling resistance = 3.1 GΩ, image size: 1 μm × 1 μm), (B) underlying surface structure (tunneling resistance = 27.5 MΩ, image size 100 nm × 100 nm), and (C) cross section through area shown in (B).

4. Conclusion

We have determined the thickness and optical constants of a self-assembled monolayer of conjugated molecules using multiple-angle spectroscopic ellipsometry. Close-packing of the molecules was indicated by ATR-FTIR spectroscopy, and the film thickness was confirmed by STM measurements. Our results show a much larger refractive index than commonly assumed for aliphatic SAMs, as expected from the conjugation of the molecules. In order to obtain accurate film thicknesses from ellipsometric data it is therefore vital to fit the thickness and the optical constants simultaneously. The accurate characterization of SAMs is crucial for their application in molecular electronics, where electrode structures must be designed to contact the molecules.

Acknowledgements

This work was supported by the European Commission IST program (IST-1999-10323, "SANEME"), the Engineering and Physical Sciences Research Council, UK, and the Danish Technical Research Council (STVF). E. M. was partly

supported by the DAAD (Deutscher Akademischer Austauschdienst).

References

[1] C.P. Collier, E.W. Wong, M. Belohradský, F.M. Raymo, J.F. Stoddart, P.J. Kuekes, R.S. Williams, J.R. Heath, Science 285 (1999) 391–394.
[2] M.A. Reed, J. Chen, A.M. Rawlett, D.W. Price, J.M. Tour, Appl. Phys. Lett. 78 (2001) 3735–3737.
[3] J.M. Tour, L.R. Jones, D.L. Pearson, J.J.S. Lamba, T.P. Burgin, G.M. Whitesides, D.L. Allara, A.N. Parikh, S. Atre, J. Am. Chem. Soc. 117 (1995) 9529–9534.
[4] L.T. Cai, Y.X. Yao, J.P. Yang, D.W. Price, J.M. Tour, Chem. Mater. 14 (2002) 2905–2909.
[5] L. Duan, S.J. Garrett, J. Phys. Chem. B 105 (2001) 9812–9816.
[6] K. Walzer, E. Marx, N.C. Greenham, R.J. Less, P.R. Raithby, K. Stokbro, J. Am. Chem. Soc. 126 (2004) 1229–1234.
[7] J.A. DeRose, T. Thundat, L.A. Nagahara, S.M. Lindsay, Surface Sci. 256 (1991) 102–108.
[8] M.D. Porter, T.B. Bright, D.L. Allara, C.E.D. Chidsey, J. Am. Chem. Soc. 109 (1987) 3559–3568.
[9] T. Baum, S. Ye, K. Uosaki, Langmuir 15 (1999) 8577–8579.
[10] S.W. Joo, S.W. Han, K. Kim, Langmuir 16 (2000) 5391–5396.
[11] E. Marx, D.S. Ginger, K. Walzer, K. Stokbro, N.C. Greenham, Nano Lett. 2 (2002) 911–914.
[12] C.M. Ramsdale, N.C. Greenham, Adv. Mater. 14 (2002) 212–215.